

## Supplementary Materials

to the manuscript "Class A GPCRs increase their sensitivity and selectivity by harnessing the energy of membrane potential"

by D. N. Shalaeva, D. A. Cherepanov, M. Y. Galperin, G.Vriend, and A. Y. Mulkidjanian

**Table S1. Experimental data on voltage-sensitive activation of GPCRs.**

Receptor	Agonist	Agonist characterization	Voltage effect on activation	Method of activity measurement	Reference
M2 muscarinic receptor	acetylcholine	full agonist (endogenous)	enhanced	GIRK currents	[1, 2]
M2 muscarinic receptor	oxotremorine	full/strong agonist	enhanced		
M1 muscarinic receptor	acetylcholine	full agonist (endogenous)	decreased		
M2 muscarinic receptor	acetylcholine	full agonist (endogenous)	enhanced	GIRK currents	[3]
M2 muscarinic receptor	acetylcholine	full agonist (endogenous)	enhanced	ACh-activated K <sup>+</sup> current	[2, 4]
M2 muscarinic receptor	pilocarpine	partial agonist	decreased		
M2 muscarinic receptor	acetylcholine	full agonist (endogenous)	enhanced	ACh-activated K <sup>+</sup> current	[2, 5] [6]
M2 muscarinic receptor	pilocarpine	partial agonist	decreased		
M2 muscarinic receptor	bethanechol	Agonist (low affinity)	no effect		
M1 muscarinic receptor	carbachol	full/strong agonist	decreased	FRET-based assays	[2, 7]
M3 muscarinic receptor	carbachol	full/strong agonist	enhanced		
mGluR3 glutamate receptor	glutamate	full agonist (endogenous)	enhanced	K <sup>+</sup> and Cl <sup>-</sup> currents	[8]
mGluR1a glutamate receptor	glutamate	full agonist (endogenous)	decreased		
$\alpha_{2A}$ -AR adrenergic receptor	noradrenaline	full agonist (endogenous)	enhanced	FRET-based assays	[9]

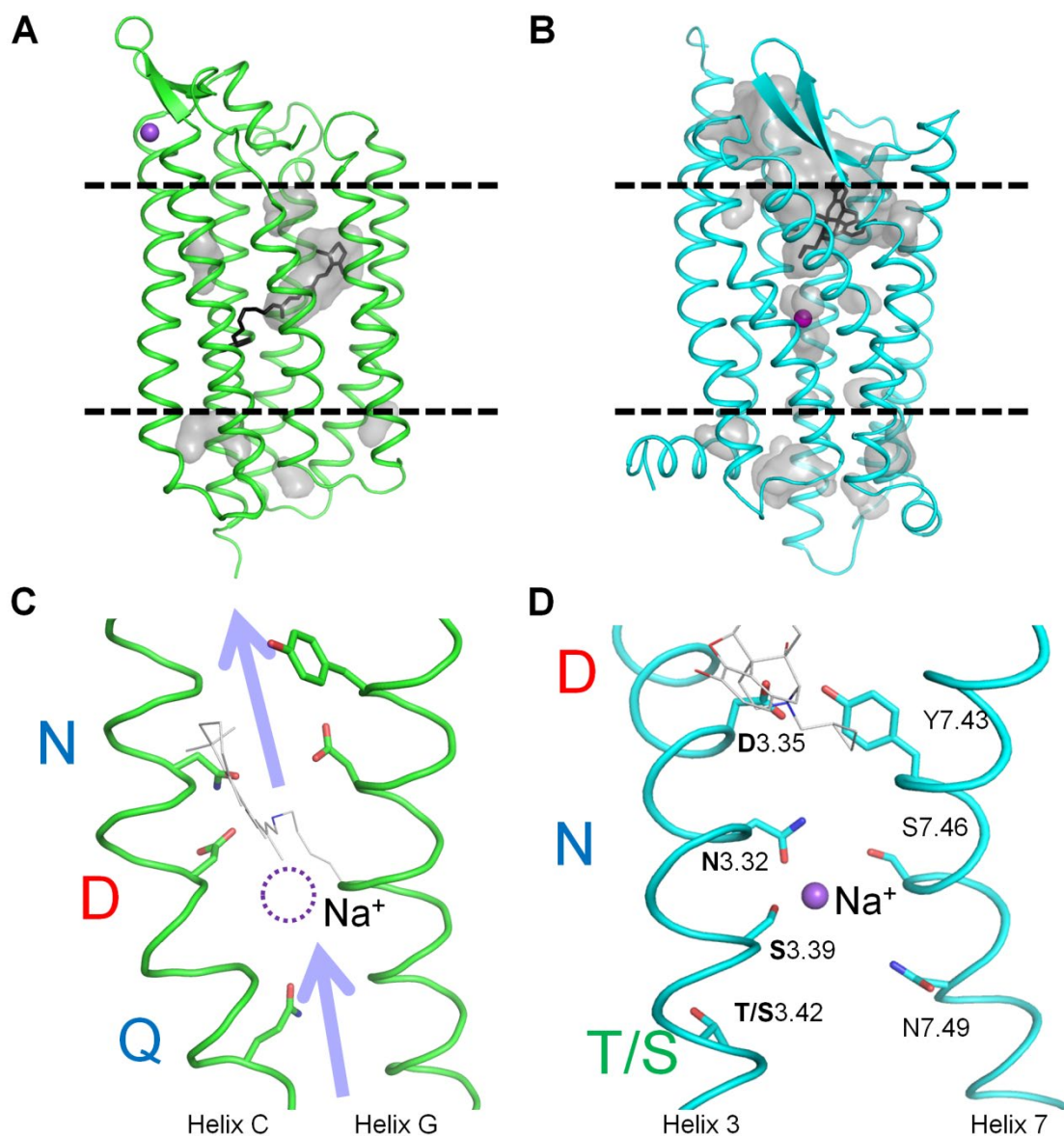
$\beta_1$ -AR adrenergic receptor	isoprenaline	full agonist	enhanced	FRET-based assays	[10, 11]
$\beta_1$ -AR adrenergic receptor	adrenaline	full agonist (endogenous)	enhanced		
dopamine D2L receptor	dopamine	full agonist (endogenous)	enhanced	GIRK currents	[12, 13]
dopamine D2L receptor	quinpirole	full agonist	enhanced		
dopamine D2S receptor	dopamine	full agonist (endogenous)		GIRK currents	[14]
dopamine D2S receptor	dopamine	full agonist (endogenous)	enhanced	GIRK currents	[12, 15]
dopamine D2S receptor	<i>p</i> -tyramine	partial agonist	decreased		
dopamine D2S receptor	<i>m</i> -tyramine	partial agonist	decreased		
dopamine D2S receptor	phenylamine	partial agonist	decreased		
dopamine D2S receptor	S-5-OH-DPAT	full agonist	no effect		
dopamine D2S receptor	R-5-OH-DPAT	full/strong agonist[16]	no effect		
dopamine D2S receptor	R-7-OH-DPAT	full/strong agonist	no effect		
dopamine D2S receptor	RIS-OH-DPAT	full/strong agonist[12]	no effect		

The effectiveness of a signaling molecule in the receptor activation does not necessarily reflect the affinity of that molecule to the receptor. Some partial agonists have a high binding affinity but induce lower receptor activity even when added in saturating amounts [2, 15]. Such molecules are believed to stabilize the receptor in an intermediate state and/or stimulate the transition to the active state with lower probability than full agonists.

1 **Table S2. Conservation of functionally important residues in Class A GPCRs.**

Residue in M <sub>2</sub> muscarinic acetylcholine receptor (PDB: 3UON)	Generic number	Most common residue		Second most common residue		Residue type, %
		AA	%	AA	%	
Na <sup>+</sup> coordination						
Asn41	1.50	N	98	S	1	Polar, 100
Asp69	2.50	D	92	N	3	Polar, 98
Ser110	3.39	S	72	T	8	Polar, 83
Trp400	6.48	W	68	F	16	Aromatic, 87
Asn432	7.45	N	67	S	11	Polar, 93
Ser433	7.46	S	64	C	13	Polar, 72
CWxP motif						
Thr399	6.47	C	71	S	10	Small, 86
Trp400	6.48	W	68	F	16	Aromatic, 87
Pro402	6.50	P	99	N/A A	N/A	Helix kink, 99
Hydrophobic shell around the Na <sup>+</sup> pocket						
Leu65	2.46	L	90	M	4	Hydrophobic, 99
Val111	3.40	I	40	V	24	Hydrophobic, 88
Leu114	3.43	L	73	I	10	Hydrophobic, 98
Ile117	3.46	I	56	L	16	Hydrophobic, 99
Ile392	6.40	V	37	I	28	Hydrophobic, 93
Leu393	6.41	V	41	L	20	Hydrophobic, 91
Phe396	6.44	F	75	V	4	Hydrophobic, 92
Second hydrophobic shell						
Val44	1.53	V	65	A	14	Hydrophobic, 92
Ile62	2.43	L	36	I	35	Hydrophobic, 97
Trp148	4.50	W	96	F	1	Hydrophobic, 99
Pro198	5.50	P	79	V	5	Hydrophobic, 95
Met202	5.54	I	33	M	30	Hydrophobic, 90
Tyr206	5.58	Y	72	S	5	Hydrophobic, 86
Ile389	6.37	L	38	V	21	Hydrophobic, 91
NPxxY motif						
Asn436	7.49	N	72	D	20	Polar, 98
Pro437	7.50	P	94	A	2	Hydrophobic, 98
Tyr440	7.53	Y	89	F	4	Aromatic, 93
DRY motif (ionic lock)						
Asp120	3.49	D	64	E	21	Polar, 97
Arg121	3.50	R	95	H	1	Polar, 98
Tyr122	3.51	Y	66	F	10	Hydrophobic, 87
Glu382	6.30	E	26	K	15	Polar, 79

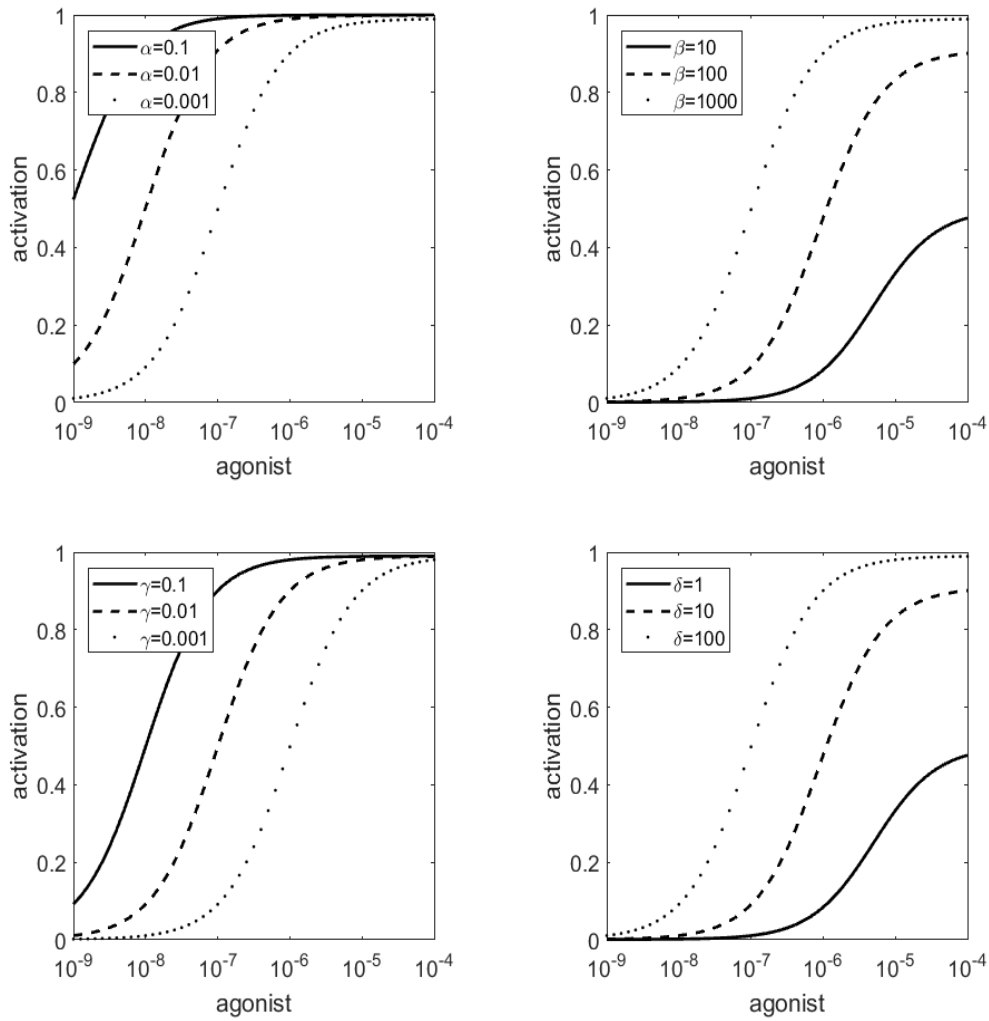
2 Residue conservation is presented as obtained from the alignment of human Class A (Rhodopsin-like) GPCRs in  
 3 the GPCRdb database [17] (not including olfactory receptors). Locations of the functionally relevant residues in  
 4 the protein structure are shown in Fig. 1.



5

6 **Figure S1. Structural and functional similarities between microbial rhodopsins (MRs)**  
 7 **and GPCRs.** **A.** Structure of sodium-translocating rhodopsin KR2 (PDB 6RF6 [18]); the  
 8 protein is shown as a cartoon, Lys255 and retinal are shown as black sticks, cavities inside  
 9 the protein are shown as gray volumes. **B.** Structure of the human  $\delta$ -opioid receptor  $\delta$ -OR  
 10 (PDB 4N6H [19]); the protein is shown as a cartoon, antagonist (naltrindole) is shown as  
 11 black sticks, cavities inside the protein are shown as gray volumes.. **C.** Signature residues  
 12 involved in cation translocation by  $\text{Na}^+$ -transporting rhodopsin KR2 (panel A). Signature  
 13 residues of the NDQ motif are shown as sticks; Lys255 and retinal are shown in gray.  
 14 Predicted  $\text{Na}^+$ -binding site is indicated by a dotted circle. **D.** Corresponding residues in  
 15 helices TM3 and TM7 in  $\delta$ -OR (panel B), antagonist (naltrindole) shown in gray, residue  
 16 numbering is according to Ballesteros-Weinstein [20].

17



19

20

21 **Figure S2. Effects of allosteric parameters  $\alpha, \beta, \gamma$  and  $\delta$  on the activation curves.**

22 Dependence of the GPCR activation on the coefficient  $\alpha$ , intrinsic efficacy of sodium (A);

23 coefficient  $\beta$ , intrinsic efficacy of the agonist (B); coefficient  $\gamma$ , binding cooperativity

24 between sodium and the agonist (C), and coefficient  $\delta$ , activation cooperativity between

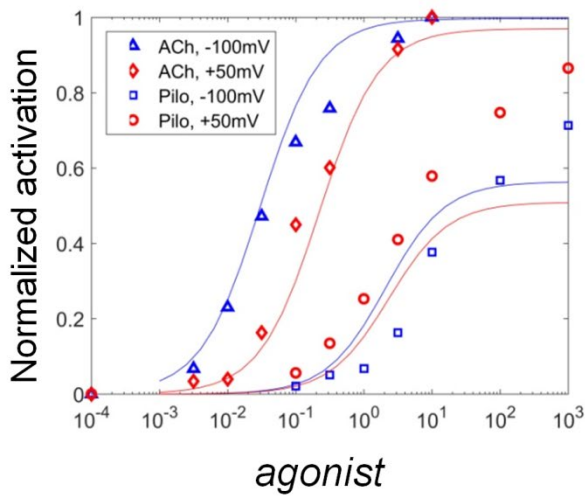
25 sodium and the agonist (D). In each panel, one of parameters was varied while the values of

26 other parameters were taken from Table 2. The impact of the membrane voltage was not

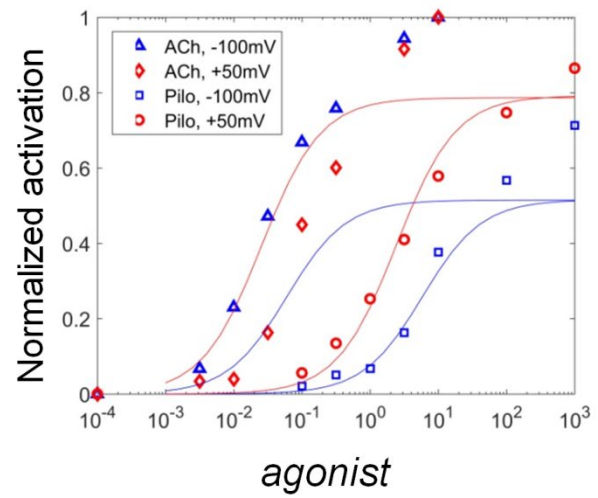
27 taken into account in the calculations.

28

### A. Mode 1: carrier-on



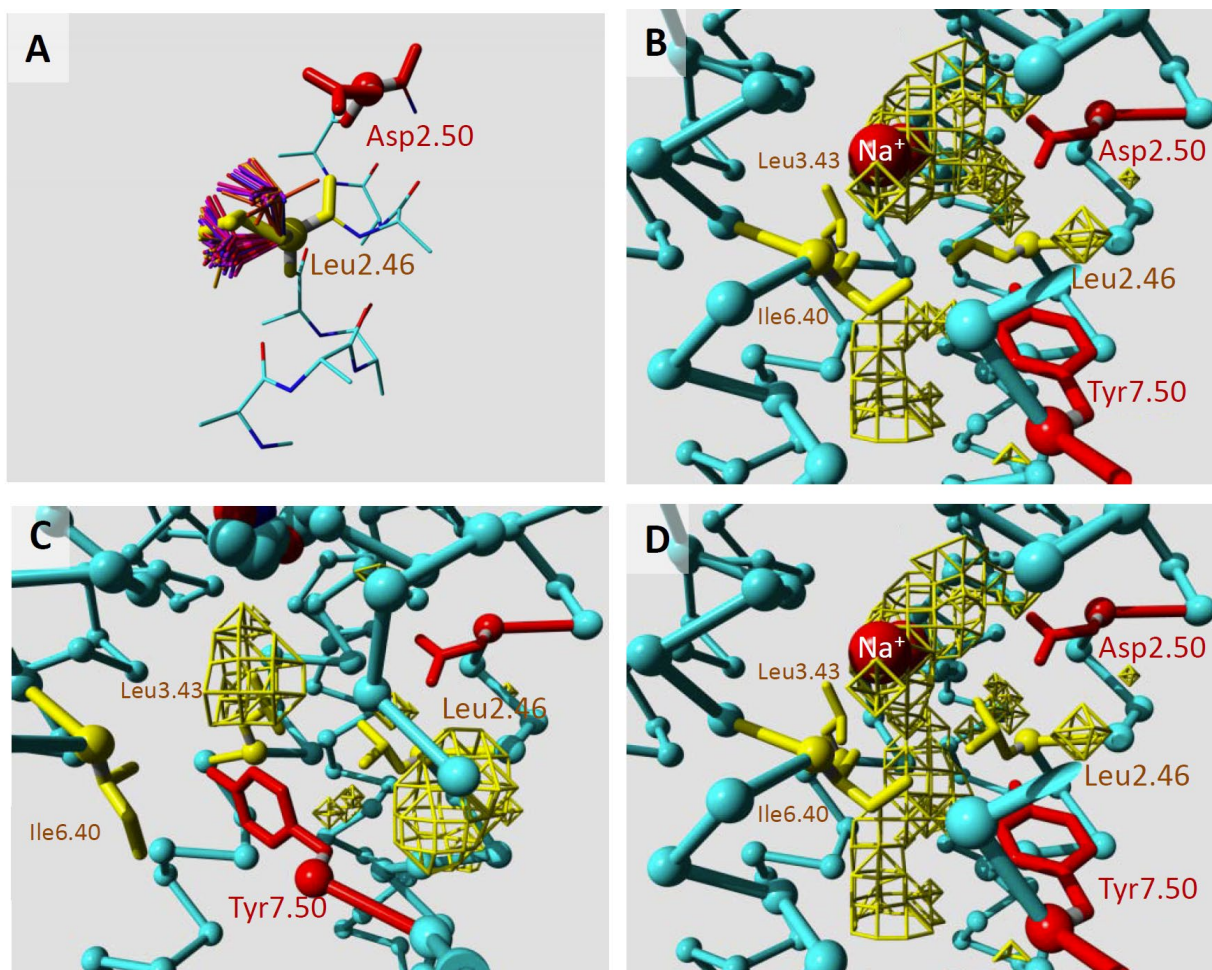
### B. Mode 2: carrier-off



29

30 **Figure S3. Fitting experimental data of voltage-sensitive muscarinic acetylcholine**  
31 **receptor M<sub>2</sub> activation.** Concentration-response curves, as obtained for the full endogenous  
32 agonist acetylcholine (ACh) and partial synthetic agonist pilocarpine (Pilo), measured at  
33 different magnitudes of membrane potential were fitted for the carrier-on mode (A) and  
34 carrier-off mode (B). Experimental data from [4].

35



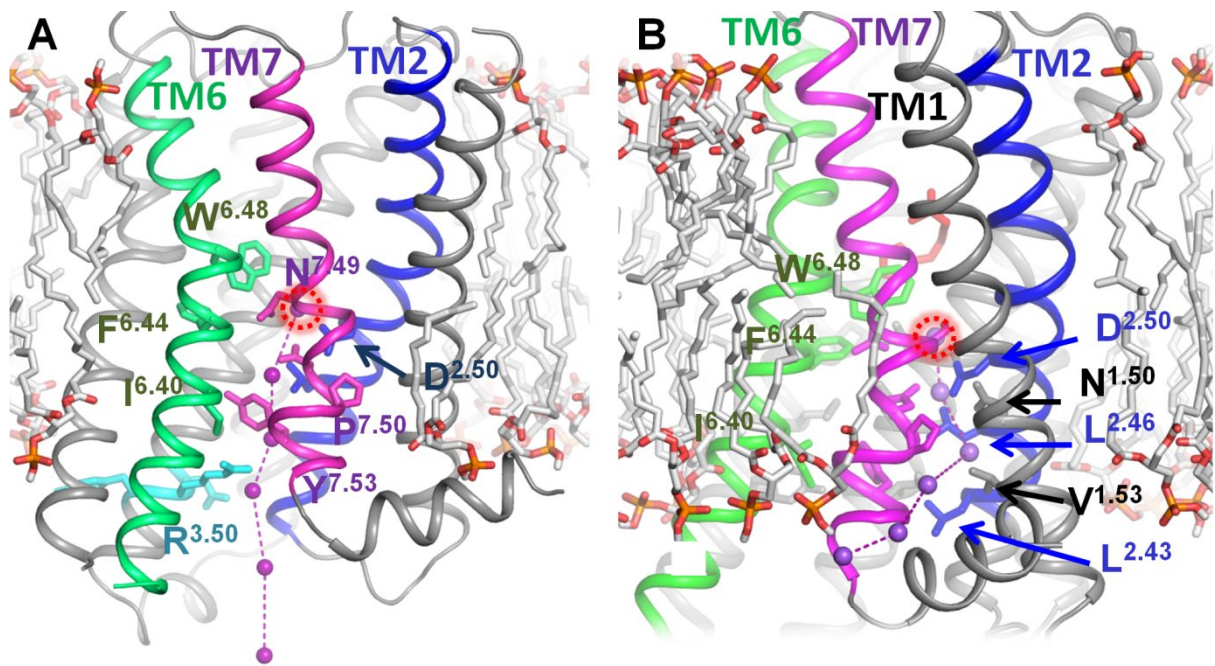
36

37 **Figure S4. Rotamers of Leu2.46 in the inactive and inactive conformations of**  
 38 **muscarinic acetylcholine receptor M<sub>2</sub>.** **A**, Analysis of Leu2.46 rotamers, shown on the  
 39 example of PDB 3UON. The section of Helix 2 is shown coloured by atom type. The  
 40 Asp2.50 side chain is shown in red. Leu2.46 as in the 3UON structure is shown in yellow.  
 41 The preferable rotamers for leucine at position 2.46 are shown in different shades of orange,  
 42 blue, and red. **B-D**, The Na<sup>+</sup> binding site in the structure of the inactive receptor, PDB 3UON  
 43 (**B**); the active receptor (PDB 4MQT) (**C**), and the inactive receptor (PDB 3UON) with  
 44 Leu2.46 moved into upper rotamer (**D**). C-alpha traces are shown in light-blue (some residues  
 45 in the front that obscured the view have been removed from the plots). Side chains of  
 46 Asp2.50 and Tyr7.50 are shown as red stick models. Cavities large enough to hold water  
 47 molecules are represented by yellow mesh. The side chains of the three aliphatic residues  
 48 Leu2.46, Leu3.43, and Ile6.40, are shown as yellow stick models.

49

50





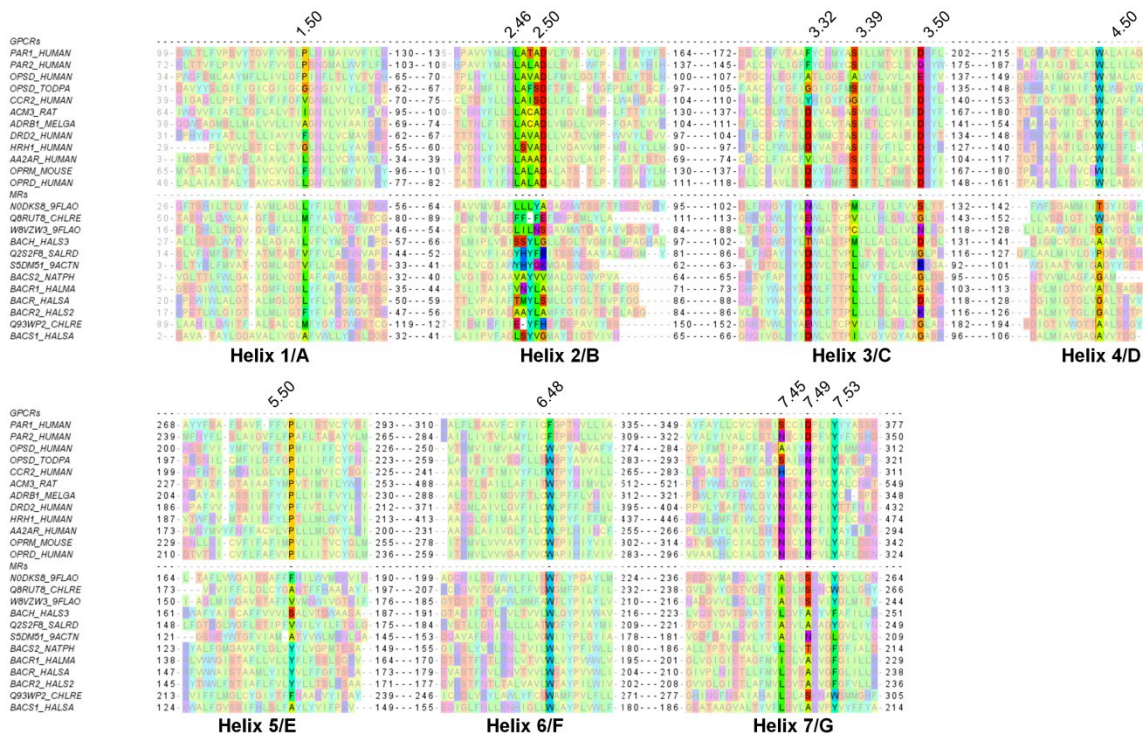
51

52 **Figure S5. Suggested pathways of Na<sup>+</sup> escape to the cytoplasm upon GPCR activation,**  
 53 **based on the structure of the M<sub>2</sub> receptor (PDB: 4MQT).** A. Putative exit pathway for the  
 54 Na<sup>+</sup> ion via the center of the heptahelical bundle. B. An alternative exit pathway via the  
 55 pocket between helices 1, 2, and 7. Helices 2, 6, and 7 are colored blue, green and purple,  
 56 respectively; conserved residues listed in Table S2 are shown as sticks. The ionic lock  
 57 residues are shown in cyan. CHARM-GUI software [21] was applied to construct the lipid  
 58 molecules of the membrane surrounding the receptors (shown as grey sticks).

59

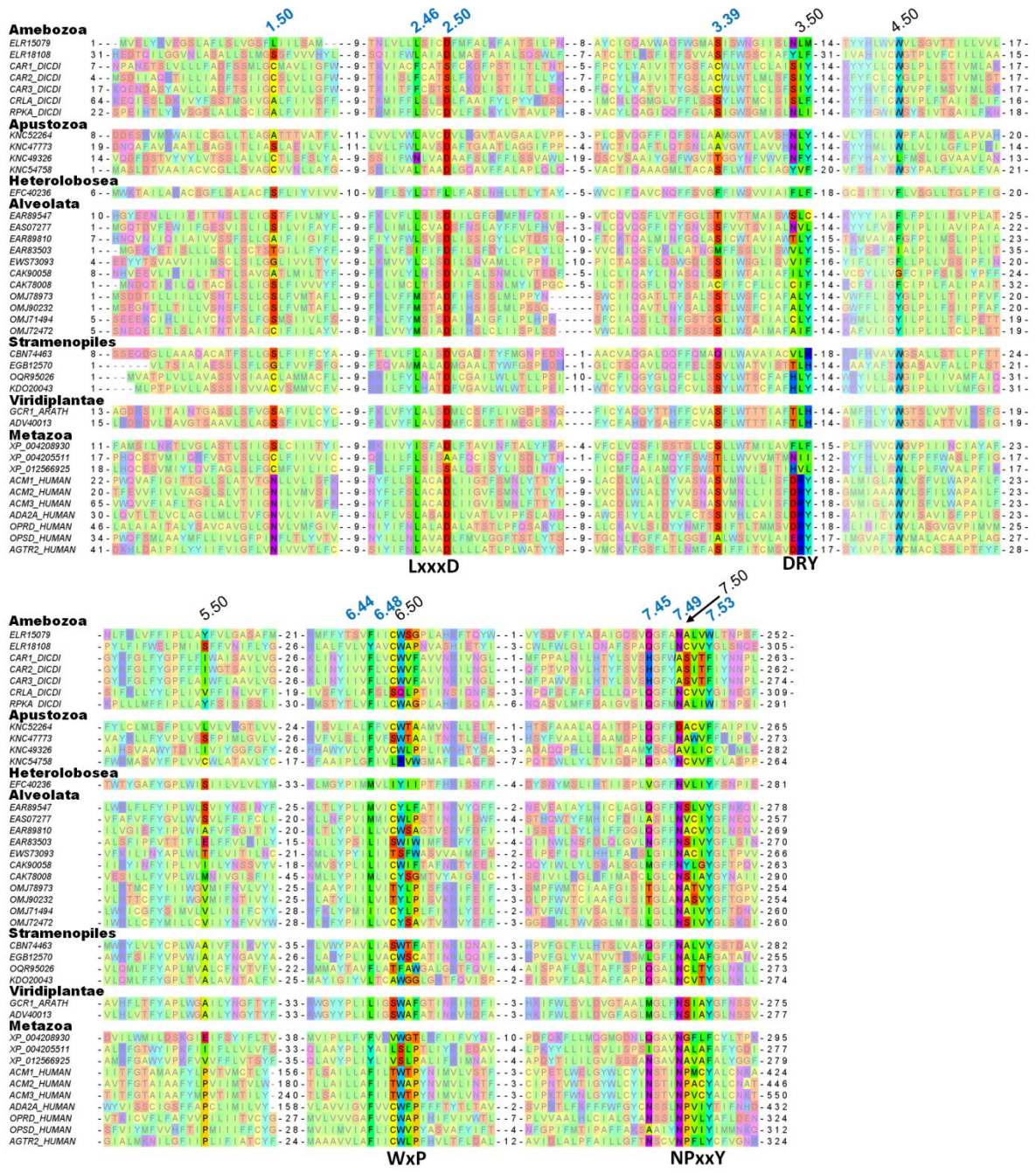
60





61  
62 **Fig. S6. Multiple sequence alignment of transmembrane segments in GPCRs and MRs.**  
63 Sequences used in the alignment (listed under their UniProt IDs): PAR1\_HUMAN - Human  
64 proteinase-activated receptor 1; PAR2\_HUMAN - Human proteinase-activated receptor 2;  
65 OPSD\_HUMAN - Human visual rhodopsin; OPSD\_TODPA - Squid visual rhodopsin;  
66 CCR2\_HUMAN - Human C-C chemokine receptor type 2; ACM3\_RAT - Rat muscarinic  
67 acetylcholine receptor M3; ADRB1\_MELGA - Turkey  $\beta$ -1 adrenergic receptor;  
68 DRD2\_HUMAN - Human D<sub>2</sub> dopamine receptor; HRH1\_HUMAN - Human histamine H1  
69 receptor; AA2AR\_HUMAN - Human adenosine receptor A2a; OPRM\_MOUSE - Mouse  $\mu$ -  
70 type opioid receptor; OPRD\_HUMAN - Human  $\delta$ -type opioid receptor. MRs:  
71 N0DKS8\_9FLAO - Sodium pumping rhodopsin from *Dokdonia eikasta*; Q8RUT8\_CHLRE -  
72 Channelrhodopsin 2 from *Chlamydomonas reinhardtii*; W8VZW3\_9FLAO - Chloride  
73 pumping rhodopsin from *Nonlabens marinus*; BACH\_HALS3 - Halorhodopsin from  
74 *Halobacterium salinarum*; Q2S2F8\_SALRD - Xanthorhodopsin from *Salinibacter ruber*;  
75 S5DM51\_9ACTN - Bacteriorhodopsin from Candidatus *Actinomarina minuta*;  
76 BACS2\_NATPH - Sensory rhodopsin-2 from *Natronomonas pharaonis*; BACR1\_HALMA -  
77 Bacteriorhodopsin-I from *Haloarcula marismortui*; BACR\_HALSA - Bacteriorhodopsin  
78 from *Halobacterium salinarum*; BACR2\_HALS2 - Archaeorhodopsin-2 from *Halobacterium*  
79 *sp.*; Q93WP2\_CHLRE - Archaeal-type opsin 1 from *Chlamydomonas reinhardtii*;  
80 BACS1\_HALSA - Sensory rhodopsin-1 from *Halobacterium salinarum*. Alignment of  
81 GPCRs was taken from the GPCRdb web service [18], alignment of MRs was constructed  
82 with T-Coffee[19], two alignments were merged using the structure superposition of human  
83  $\delta$ -opioid receptor (PDB 4N6H) and channelrhodopsin 2 from *Chlamydomonas reinhardtii*  
84 (PDB 6EIG), as described in [20].  
85





86

87 **Figure S7. Multiple sequence alignment of class A GPCRs from primitive organisms (the full version of**  
 88 **the Fig. 5 of the main text).** Sequences are listed under their GenBank, UniProt or RefSeq accessions and are  
 89 as follows: Amebozoa: phosphatidylinositol 4-phosphate 5-kinase protein from *Acanthamoeba castellanii*  
 90 (GenBank: ELR15079); cAMP receptor protein from *Acanthamoeba castellanii* (GenBank: ELR18108); cAMP  
 91 receptor 1 from *Dictyostelium discoideum* (UniProt: CAR1\_DICDI); cAMP receptor 2 from *Dictyostelium*  
 92 *discoideum* (UniProt: CAR2\_DICDI); cAMP receptor 3 from *Dictyostelium discoideum* (UniProt:  
 93 CAR3\_DICDI); cAMP receptor-like protein from *Dictyostelium discoideum* (UniProt: CAR4\_DICDI), and G-  
 94 protein-coupled receptor family protein from *Dictyostelium discoideum* (UniProt: RPKA\_DICDI). Apustozoa:  
 95 hypothetical protein MSG\_01092 from *Thecamonas trahens* (GenBank: KNC52264); hypothetical protein  
 96 MSG\_04000 from *Thecamonas trahens* (GenBank: KNC47773); hypothetical protein MSG\_02398 from  
 97 *Thecamonas trahens* (GenBank: KNC56428); PPK-1 protein from *Thecamonas trahens* (GenBank:  
 98 KNC49326); hypothetical protein MSG\_01609 from *Thecamonas trahens* (GenBank: KNC54758).  
 99 Heterolobosea: predicted protein NAEGRDRAFT\_72027 from *Naegleria gruberi* (GenBank: EFC40236).  
 100 Alveolata: G protein coupled glucose receptor from *Tetrahymena thermophila* (GenBank: EAR89547); 7TM  
 101 secretin family protein from *Tetrahymena thermophila* (GenBank: EAS07277); 7TM secretin family protein

102 from *Tetrahymena thermophila* (GenBank: EAR89810); G protein coupled glucose receptor from *Tetrahymena*  
103 *thermophila* (GenBank: EAR83503); cAMP receptor from *Tetrahymena thermophila* (GenBank: EWS73093);  
104 unnamed protein product from *Paramecium tetraurelia* (GenBank: CAK90058); hypothetical protein from  
105 *Paramecium tetraurelia* (Genbank: CAK78008); hypothetical protein SteCoe\_21100 from *Stentor coeruleus*  
106 (GenBank: OMJ78973); hypothetical protein SteCoe\_30276 from *Stentor coeruleus* (GenBank: OMJ71494);  
107 hypothetical protein SteCoe\_7430 from *Stentor coeruleus* (GenBank: OMJ90232); hypothetical protein  
108 SteCoe\_29065 from *Stentor coeruleus* (GenBank: OMJ72472). Stramenopiles: G-protein coupled receptor from  
109 *Ectocarpus siliculosus* (GenBank: CBN74463); hypothetical protein AURANDRAFT\_4432 from *Aureococcus*  
110 *anophagefferens*, partial (GenBank: EGB12570); hypothetical protein ACHHYP\_00504 from *Achlya hypogyna*  
111 (GanBank: OQR95026); hypothetical protein SPRG\_14191 from *Saprolegnia parasitica* (GenBank:  
112 KDO20043). Viridiplantae: G-protein coupled receptor 1 from *Arabidopsis thaliana* (UniProt: GCR1\_ARATH);  
113 G protein coupled receptor from *Oryza sativa* (GenBank: ADV40013). Metazoa: predicted probable G-protein  
114 coupled receptor 157 from *Hydra vulgaris*, partial (NCBI RefSeq: XP\_004208930); predicted cAMP receptor-  
115 like protein A from *Hydra vulgaris* (NCBI RefSeq: XP\_004205511); predicted G-protein coupled receptor 1-  
116 like protein from *Hydra vulgaris* (NCBI RefSeq: XP\_012566925); human muscarinic acetylcholine receptor M<sub>1</sub>  
117 (UniProt: ACM1\_HUMAN); human muscarinic acetylcholine receptor M<sub>3</sub> (UniProt: ACM3\_HUMAN); human  
118  $\alpha_2A$  adrenergic receptor (UniProt: ADA2A\_HUMAN); human  $\delta$ -type opioid receptor (UniProt:  
119 OPRD\_HUMAN); human visual rhodopsin (UniProt: OPSD\_HUMAN).

120

121 **References**

- 122 [1] Y. Ben-Chaim, O. Tour, N. Dascal, I. Parnas, H. Parnas, The M2 muscarinic G-protein-coupled  
123 receptor is voltage-sensitive, *J. Biol. Chem.*, 278 (2003) 22482-22491.
- 124 [2] M.H. Richards, P.L. van Giersbergen, Human muscarinic receptors expressed in A9L and CHO  
125 cells: activation by full and partial agonists, *Br J Pharmacol*, 114 (1995) 1241-1249.
- 126 [3] Y. Ben-Chaim, B. Chanda, N. Dascal, F. Bezanilla, I. Parnas, H. Parnas, Movement of 'gating  
127 charge' is coupled to ligand binding in a G-protein-coupled receptor, *Nature*, 444 (2006) 106-109.
- 128 [4] R.A. Navarro-Polanco, E.G. Moreno Galindo, T. Ferrer-Villada, M. Arias, J.R. Rigby, J.A.  
129 Sanchez-Chapula, M. Tristani-Firouzi, Conformational changes in the M2 muscarinic receptor  
130 induced by membrane voltage and agonist binding, *J Physiol*, 589 (2011) 1741-1753.
- 131 [5] E.G. Moreno-Galindo, J. Alamilla, J.A. Sanchez-Chapula, M. Tristani-Firouzi, R.A. Navarro-  
132 Polanco, The agonist-specific voltage dependence of M2 muscarinic receptors modulates the  
133 deactivation of the acetylcholine-gated K(+) current (I KACH), *Pflugers Arch*, 468 (2016) 1207-1214.
- 134 [6] R.A. Copeland, Drug-target residence time, in: G.M. Keseru (Ed.) *Thermodynamics and Kinetics*  
135 *of Drug Binding*, Wiley-VCH Verlag GmbH, 2015, pp. 157-167.
- 136 [7] A. Rinne, J.C. Mobarec, M. Mahaut-Smith, P. Kolb, M. Bunemann, The mode of agonist binding  
137 to a G protein-coupled receptor switches the effect that voltage changes have on signaling, *Sci Signal*,  
138 8 (2015).
- 139 [8] L. Ohana, O. Barchad, I. Parnas, H. Parnas, The metabotropic glutamate G-protein-coupled  
140 receptors mGluR3 and mGluR1a are voltage-sensitive, *J. Biol. Chem.*, 281 (2006) 24204-24215.
- 141 [9] A. Rinne, A. Birk, M. Bunemann, Voltage regulates adrenergic receptor function, *Proc. Natl.*  
142 *Acad. Sci. USA*, 110 (2013) 1536-1541.
- 143 [10] A. Birk, A. Rinne, M. Bunemann, Membrane Potential Controls the Efficacy of Catecholamine-  
144 induced beta1-Adrenoceptor Activity, *J. Biol. Chem.*, 290 (2015) 27311-27320.
- 145 [11] G. Lebon, T. Warne, P.C. Edwards, K. Bennett, C.J. Langmead, A.G.W. Leslie, C.G. Tate,  
146 Agonist-bound adenosine A(2A) receptor structures reveal common features of GPCR activation,  
147 *Nature*, 474 (2011) 521-U154.
- 148 [12] K. Sahlholm, D. Marcellino, J. Nilsson, K. Fuxe, P. Arhem, Differential voltage-sensitivity of  
149 D2-like dopamine receptors, *Biochem. Biophys. Res. Commun.*, 374 (2008) 496-501.
- 150 [13] R.A. Copeland, The drug-target residence time model: a 10-year retrospective, *Nat Rev Drug*  
151 *Discov*, 15 (2016) 87-95.
- 152 [14] K. Sahlholm, O. Barchad-Avitzur, D. Marcellino, M. Gomez-Soler, K. Fuxe, F. Ciruela, P.  
153 Arhem, Agonist-specific voltage sensitivity at the dopamine D2S receptor--molecular determinants  
154 and relevance to therapeutic ligands, *Neuropharmacology*, 61 (2011) 937-949.
- 155 [15] R.A. Copeland, Conformational adaptation in drug-target interactions and residence time, *Future*  
156 *Med Chem*, 3 (2011) 1491-1501.
- 157 [16] K. Sahlholm, J. Nilsson, D. Marcellino, K. Fuxe, P. Arhem, Voltage-dependence of the human  
158 dopamine D2 receptor, *Synapse*, 62 (2008) 476-480.
- 159 [17] V. Isberg, B. Vroiling, R. van der Kant, K. Li, G. Vriend, D. Gloriam, GPCRDB: an information  
160 system for G protein-coupled receptors, *Nucleic Acids Res.*, 42 (2014) D422-D425.
- 161 [18] K. Kovalev, V. Polovinkin, I. Gushchin, A. Alekseev, V. Shevchenko, V. Borshchevskiy, R.  
162 Astashkin, T. Balandin, D. Bratanov, S. Vaganova, A. Popov, V. Chupin, G. Buldt, E. Bamberg, V.  
163 Gordeliy, Structure and mechanisms of sodium-pumping KR2 rhodopsin, *Sci Adv*, 5 (2019)  
164 eaav2671.
- 165 [19] G. Fenalti, P.M. Giguere, V. Katritch, X.P. Huang, A.A. Thompson, V. Cherezov, B.L. Roth,  
166 R.C. Stevens, Molecular control of delta-opioid receptor signalling, *Nature*, 506 (2014) 191-196.
- 167 [20] J.A. Ballesteros, H. Weinstein, Integrated methods for the construction of three-dimensional  
168 models and computational probing of structure-function relations in G protein-coupled receptors, in:  
169 *Methods in Neurosciences*, Elsevier, 1995, pp. 366-428.
- 170 [21] S. Jo, T. Kim, V.G. Iyer, W. Im, CHARMM-GUI: a web-based graphical user interface for  
171 CHARMM, *J. Comput. Chem.*, 29 (2008) 1859-1865.